

RESEARCH MEMORANDUM

EFFECT OF INLET-AIR BAFFLES ON ROTATING-STALL AND STRESS

CHARACTERISTICS OF AN AXIAL-FLOW COMPRESSOR

IN A TURBOJET ENGINE

By S. C. Huntley, Merle C. Huppert, and Howard F. Calvert

Lewis Flight Propulsion Laboratory Cleveland, Ohio

CASE FILE

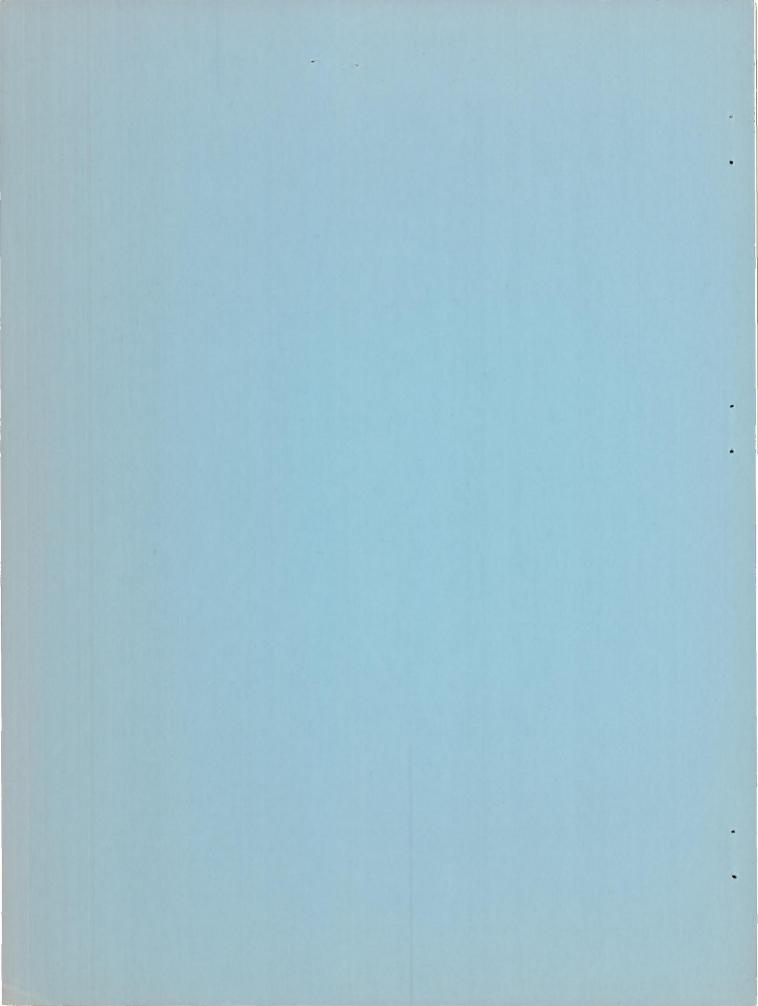
CLASSIFIED DOCUMENT

This material contains information affecting the National Defense of the United States within the meaning of the espionage laws, Title 18, U.S.C., Secs. 793 and 794, the transmission or revelation of which in any

NATIONAL ADVISORY COMMITTEE FOR AERONAUTICS

> WASHINGTON January 10, 1955

for Aeromanties Washington, D. C.



NATIONAL ADVISORY COMMITTEE FOR AERONAUTICS

RESEARCH MEMORANDUM

EFFECT OF INLET-AIR BAFFLES ON ROTATING-STALL AND STRESS
CHARACTERISTICS OF AN AXIAL-FLOW COMPRESSOR

IN A TURBOJET ENGINE

By S. C. Huntley, Merle C. Huppert, and Howard F. Calvert

SUMMARY

The effect of inlet-air baffles on the rotating stall, the rotor-blade vibratory stress, and the performance characteristics of a compressor were determined in an axial-flow turbojet engine. Two baffle designs, consisting of annular rings, were used: (1) An inside-diameter baffle extending radially outward from the hub, and (2) an outside-diameter baffle extending radially inward from the outer casing. Each baffle blocked approximately one third of the inlet annulus area.

Either baffle successfully eliminated rotating stall and reduced vibratory stress measured in the inlet-stage rotor blades from ±26,000 to ±5000 pounds per square inch. Compressor efficiency was reduced from 11 to 15 percentage points for engine speeds of 60 to 75 percent of rated speed; pressure ratio and corrected air flow were also reduced. This loss in performance may be reduced by optimizing baffle size and by modulating baffle size as a function of engine speed.

INTRODUCTION

One of the troublesome problems encountered in the development of many turbojet engines is compressor blade vibration and fatigue failure. Several investigations (refs. 1 to 3) have indicated that one source of blade vibration can be the periodic flow fluctuations associated with rotating stall. The occurrence of rotating stall at low and intermediate engine speeds can be attributed to the fact that the design ratio of compressor inlet to exit area is too large to permit all stages to operate at some off-design conditions without stall. Flow limitations, imposed by the exit stages of the compressor at low engine speed, usually result in rotating stall being instigated in the inlet stages (ref. 4).

It has been suggested that reducing the compressor-inlet area at low speed may alleviate the periodic flow fluctuations associated with rotating stall and, hence, this source of blade excitation. An

investigation on a compressor unit (ref. 5) indicated that inlet-area blockage would be an effective means of removing the periodicity of the stall patterns. Inasmuch as vibratory stresses were not measured, reference 5 did not indicate the extent of stress-level reduction resulting from the use of inlet-area blockage. The turbojet engine discussed in reference 1 had large compressor-blade vibratory stresses due to rotating stall, and was therefore well suited to a determination of the effectiveness of baffles in reducing the stresses caused by rotating stall. The object of the investigation reported herein was to determine the effect of inlet-air baffles on the rotating-stall and vibratory-stress characteristics of the compressor operating in a later version of the turbojet engine described in reference 1.

The investigation was conducted in an altitude test chamber at the NACA Lewis laboratory. Two separate baffle designs were used; each baffle blocked approximately one third of the inlet annulus area at either the inner or outer diameter. A comparison is made between the rotating-stall and vibratory-stress characteristics of the compressor with and without baffles. In addition, the effect of the baffles on compressor performance is presented. The relative quasi-static acceleration rates with and without baffles are also briefly discussed.

Rotating stall, blade vibration, and steady-state performance characteristics were evaluated with no baffle and with each baffle over a range of speeds from 60 to 75 percent of rated engine speed at conditions approximating static sea level. Several exhaust-nozzle areas were used to obtain different engine operating lines. Constant-current hot-wire anemometers were used in the first three compressor stages to detect the flow fluctuations of rotating stall. Resistance-wire strain gages were used in the first three rotor-blade rows to detect and to measure blade vibrations. Steady-state pressures and temperatures were also measured at several stations throughout the compressor.

APPARATUS

Engine and installation. - The investigation was conducted in an NACA Lewis altitude test chamber using a turbojet engine having an 13-stage axial-flow compressor with a pressure ratio of about 7. Several exhaust-nozzle areas were used to obtain a range of engine operating lines. The exhaust-nozzle areas used covered the range from the area required to obtain compressor pressure ratios associated with normal engine operation to the area required to reach limiting exhaust-gas temperature at the maximum engine speed investigated (about 75 percent of rated speed).

Inlet-air baffles. - Two baffle configurations supplied by the engine manufacturer were used. A photograph of each baffle and schematic views of baffle locations are shown in figure 1. Each baffle consisted

of an annular plate located ahead of the inlet guide vanes and extending from either the outer or inner wall. The physical flow area was reduced approximately one third in either case. The baffle extending from the outer wall, hereinafter called the O.D. baffle, was approximately 1/16 inch thick, extended $1\frac{15}{16}$ inches from the outer wall, and was located $1\frac{1}{8}$ inches ahead of the inlet guide vanes. The other baffle, hereinafter called the I.D. baffle, was 1/4 inch thick, extended $3\frac{1}{16}$ inches from the inner wall, and was located 11/16 inch ahead of the inlet guide vanes.

Instrumentation. - A cross section of the engine showing stations at which pressure and temperature instrumentation was installed is shown in figure 2. Also shown in figure 2 are some typical station views and a table summarizing the pressure and temperature instrumentation. Pressure and temperature probes at each station were located on area centers of equal annulus areas.

Resistance-wire strain gages were cemented to 24 rotor blades in the first three stages of the compressor at the midchord position as close as possible to the blade base. The instrumented blades were equally divided among the three stages, in two diametrically opposite groups of four blades each. Lead wires were run along the hub of the compressor rotor to the first-stage disk, across the face of the first-stage disk to the center line of the compressor, and then through the shaft to a 19-ring slip-ring assembly. The slip-ring assembly and strain-gage circuits were the same as those described in reference 6.

Constant-current hot-wire anemometers were used to detect flow fluctuations. A 0.001-inch-diameter by 0.01-inch-length wire, kept at a constant average temperature, was used in each anemometer. The flow fluctuations were detected from the instantaneous variations in wire temperature. A resistance-capacitor-type compensator was used to obtain the necessary speed of response. The method used to determine rotating stall was that outlined in reference 7. Anemometer probes were installed in radial-survey devices and located in the first-, second-, and third-stage stator passages. Three angular spacings of the anemometer probes (approximately 30°, 60°, and 90°) were provided in each stage. A 24-channel recording oscillograph was used to record both the strain-gage and hot-wire-anemometer signals.

PROCEDURE

The engine was operated over a range of engine speeds from 60 to 75 percent of rated speed with each configuration for three different exhaust-nozzle areas. This range of engine speeds corresponded to the region in which rotating stall and high vibratory blade stresses were found to exist in the compressor with no baffle. Comparative data were

obtained with each configuration by use of the large exhaust-nozzle area. The exhaust-nozzle area was then decreased to obtain compressor operation over a range of compressor pressure ratios at each engine speed. The minimum exhaust-nozzle area was selected by the attainment of limiting exhaust-gas temperature at the maximum engine speed investigated. An intermediate exhaust-nozzle area was arbitrarily selected to give an exhaust-gas temperature approximately midway between the limiting value and that obtained with the large exhaust-nozzle area. Pressures, temperatures, hot-wire signals and strain-gage signals were recorded for numerous points along each operating line.

The brief exploratory nature of this investigation precluded the determination of altitude effects on compressor performance with the baffles. Atmospheric air at about 65±5° F was used and a compressorinlet total pressure of about 1900 pounds per square foot was maintained. An altitude static pressure of about 1800 pounds per square foot was maintained by the exhaust-system facilities.

The methods of calculating blade-element performance and acceleration rate used in this report are shown in the appendix.

RESULTS AND DISCUSSION

Effect of Baffles on Rotating Stall and Blade Stress

It is clearly shown in reference 1 that peak blade vibration stresses occurred in the earlier version of this compressor when the natural blade vibration frequency corresponded to a harmonic of rotating stall frequency. Therefore, in order to reduce blade vibratory stress, it is necessary to remove the periodic flow fluctuations associated with rotating stall.

A typical oscillograph record obtained at approximately 70 percent of rated speed during the investigation with and without a baffle installed is shown in figure 3. Two hot-wire traces are shown near the bottom of each record. The anemometer probes were located, in both instances, at the radial location which indicated the maximum flow fluctuations with no baffle. It may be observed that flow fluctuations with the baffle installed (fig. 3(a)) are of a random or nonperiodic nature which is in direct contrast to the periodic flow fluctuations with no baffle (fig. 3(b)). Examination of all hot-wire traces, of which figure 3(a) is typical, showed that either the I.D. or O.D. baffle eliminated the periodic flow fluctuations over the entire range of engine speed and for all nozzle areas investigated.

33

Also shown in the typical oscillograph records of figure 3 are four traces of strain-gage signals in each of the first three stages. These traces are labeled in figure 3 according to the stage in which the strain gages were located. As expected, with rotating stall eliminated by use of the baffles, the high blade stresses were also eliminated. Higher mode vibrations were indicated by higher frequency fluctuations in both instances but were more predominant with a baffle installed.

The effect of the baffles on peak vibratory stress is presented in figure 4 as a function of engine speed. The envelope of peak vibratory stress and the stage in which it occurred is shown in figure 4 for each configuration. During engine operation with no baffle, peak stresses of about ±26,000 pounds per square inch were measured at two distinct engine speeds of approximately 62 and 70 percent of rated speed for the first and second stages, respectively. With either the I.D. or 0.D. baffle installed, the peak stresses occurred in the third stage and were reduced to about ±5000 pounds per square inch. It is apparent that the baffles were effective in both eliminating rotating stall and reducing peak vibratory blade stresses.

Effect of Baffles on Compressor Performance

Pressure and temperature profiles. - Total-pressure and -temperature profiles measured in the second, fourth, and ninth stators and at the compressor outlet during engine operation with the large exhaust-nozzle area at an engine speed of approximately 60 percent of rated speed are presented in figures 5 and 6. In order to compare the profiles, the local value at each immersion depth was divided by the average value at that axial station. The effect of the baffles on these profiles may be seen by comparison with the profiles obtained with no baffle. As would be expected, the ratio of local to average total pressure in the region behind each baffle is below the corresponding ratio with no baffle (fig. 5). The influence of the baffles on the radial pressure distribution was pronounced in the second and fourth stators but became practically nullified in the ninth stator and the compressor outlet. The low air flow behind each baffle results in a low axial velocity and, therefore, high angles of attack with subsequent blade stall and high temperatures. Consequently, the ratio of local to average total temperature was higher in the region behind each baffle (fig. 6). Although the baffles had a negligible effect on the pressure profiles at the ninth stator and the compressor outlet, the influence of the baffles on the radial temperature distribution remained high throughout the compressor. Similar trends in the pressure and temperature profiles were observed at the highest engine speed investigated.

Blade-element performance. - Blade-element performance of the first two compressor stages was calculated for several immersion depths. Immersion depths directly downstream of each baffle were not considered since the flow coefficient, which is based on the inlet conditions to each element, was assumed to be zero. Under these conditions (near zero flow coefficient) it is unlikely that rotating stall could exist. A constant air flux was assumed across the unbaffled portion of the inlet annulus for the calculation of flow coefficient (see appendix). Furthermore, since large radial pressure gradients are induced by the baffles in the inlet stages (see fig. 5), flow coefficients for the baffle data must be considered only qualitative. The blade-element performance of the first two stages with baffles is presented in figure 7 for several immersion depths. Also shown is the performance of the same blade elements with no baffle. A comparison of the baffle data with that for no baffle shows that the baffles have caused the blade elements to operate with a decreasing pressure coefficient with increasing flow coefficient rather than with an increasing or constant pressure coefficient. A typical inlet-stage blade-element characteristic curve is shown in figure 8. Rotating stall in inlet stages generally is found at values of flow coefficient less than the value for peak-pressure coefficient as indicated in the curve. At flow coefficients greater than that required to give maximum pressure coefficient, angles of attack are more favorable and rotating stall is not instigated. The characteristic curves with baffles in figure 7 have a negative slope similar to the slope of the portion of the typical characteristic curve shown in figure 8 which corresponds to operation free of rotating stall. These qualtitative stage data show that the baffles eliminated rotating stall by reducing the angle of attack.

The increase in flow coefficient by the use of a fixed baffle (fig. 7) suggests the possibility of advantages from modulating baffle size to control the performance of the inlet stages. At low engine speeds, the compressor air flow is limited, when no baffles are used, by the flow area of the exit stages. The flow coefficient increases with increasing engine speed. Near the tip (low immersion depth) the blade elements with no baffle approach the peak pressure coefficient with increasing engine speed but the pressure coefficients of the same elements with a fixed baffle decreases with increasing speed. Modulating baffle size with engine speed to maintain a pressure coefficient at the tip near the peak value (at low engine speeds) should permit maximizing performance while eliminating rotating stall. The relatively low values of pressure coefficient obtained with the baffles used in this investigation are probably the result of the baffles being too large, indicating that some benefit may be realized from optimizing baffle size, location, or both.

Over-all performance. - The effect of the baffles on the over-all compressor performance is presented in figure 9 as a function of engine speed. Compressor efficiency, pressure ratio, and air flow obtained

while operating the engine with the large exhaust-nozzle area are shown. Similar compressor performance obtained with no baffle is also shown. The large exhaust-nozzle area was selected for this comparison because it was the only common one used for each configuration. A decrease in compressor efficiency from 11 to 15 points compared with the unbaffled compressor performance was obtained when either baffle was used. Compressor pressure ratio and air flow were also reduced as much as 20 percent during operation with the baffles.

The boundaries of the region of compressor operation obtained with each baffle during this investigation is presented in figure 10. Also shown are similar boundaries obtained with no baffle. The relative size and location of the enclosures shown in figure 10 graphically indicate the effect of the baffles on the over-all compressor performance.

This discussion of over-all compressor performance has indicated sizable reductions in air flow and compressor ratio by the use of the baffles of this investigation. As previously mentioned, the principal consideration in using the baffles was to eliminate rotating stall and subsequently reduce rotor-blade vibratory stresses. Obviously the baffles should be retracted at engine speeds above which rotating stall is encountered to avoid the large performance penalties shown in figures 9 and 10.

Effect of Baffles on Acceleration Characteristics

An experimental evaluation of acceleration characteristics was not within the scope of this brief exploratory investigation. A brief, simple calculation was made, however, to determine the quasi-static acceleration rates of the engine from the compressor performance maps (see appendix). A turbine-inlet pressure of 97 percent of compressor outlet pressure was assumed. The turbine-nozzle area and the exhaustnozzle area were assumed constant. The turbine was assumed to operate at a constant adiabatic efficiency of 0.85. The quasi-static acceleration rate calculated using these assumptions is presented in figure 11 as a function of the ratio of turbine inlet to engine inlet temperature. The relative acceleration rate was obtained by dividing the acceleration rate by that obtained with no baffle at a turbine-inlet temperature ratio of 3.44. An engine speed of 65 percent of rated speed was arbitrarily selected for each configuration. A lower acceleration rate at a given turbine-inlet temperature ratio was calculated for the baffles of this investigation; however, as previously discussed, these baffles were larger than necessary for the elimination of rotating stall. Decreasing baffle size would probably increase the acceleration rate at a given turbine-inlet temperature ratio. The range of acceleration rates shown in figure 11 for each configuration was limited by the extent of the available steady-state data and does not indicate the peak acceleration rate which would be limited by the stall-limit line. Although the stalllimit line was not obtained in this investigation, the data of reference 5 on a different compressor indicated an improvement in the stall-limit line and an increase in acceleration potential by the use of a baffle.

SUMMARY OF RESULTS

An investigation was conducted to determine the effectiveness of inlet-air baffles in eliminating rotating stall and reducing high vibratory blade stresses in an axial-flow compressor of a turbojet engine. Two separate baffle designs were used; each baffle blocked approximately one third of the inlet annulus area at either the inner or outer diameter. Either of the baffles successfully eliminated rotating stall and reduced vibratory stresses measured in the rotor blades of the first three stages from ±26,000 to ±5000 pounds per square inch. The baffles had a pronounced effect on radial total-pressure distribution in the second and fourth stage stators, but the effect became practically nullified in the ninth-stage stator. In the range of engine speeds from 60 to 75 percent of rated speed, the baffles decreased compressor efficiency from 11 to 15 points and also reduced both the pressure ratio and the air flow. This loss in performance may be reduced by optimizing and modulating baffle size as a function of engine speed.

Lewis Flight Propulsion Laboratory
National Advisory Committee for Aeronautics
Cleveland, Ohio, July 12, 1954

APPENDIX - METHOD OF CALCULATION

Symbols

The following symbols were used in the calculations:

A area, sq ft

Ah annulus area blocked by baffle, sq ft

A annulus area at inlet guide vanes, sq ft

cp specific heat at constant pressure, Btu/(lb)(OR)

D blade element diameter, ft

g acceleration due to gravity, ft/sec2

n number of stages

N engine speed, rpm

P total pressure, lb/sq ft

R gas constant, ft-lb/(lb)(OR)

T total temperature, OR

W air weight flow, lb/sec

γ ratio of specific heats

δ ratio of total pressure to NACA standard sea-level pressure, P/2116

η efficiency

 θ ratio of total temperature to NACA standard sea-level temperature, T/519

 ρ_{T} density based on total conditions, lb/cu ft

$$\frac{\text{Axial-air velocity}}{\text{Rotor velocity}} \approx \frac{W_1}{\rho_{t,1}(A_{igv}-A_b)} \left(\frac{\pi D_i N}{60}\right)$$

$$\frac{\text{Isentropic energy rise}}{\text{Rotor kinetic energy}}, \frac{\gamma g R T_{i}}{\gamma - 1} \left[\left(\frac{P_{o}}{P_{i}} \right)^{\gamma} - 1 \right] / n \left(\frac{\pi D_{i} N}{60} \right)^{2}$$

CONFIDENTIAL

Subscripts:

- l compressor inlet
- 3 compressor outlet
- 4 turbine inlet
- 9 exhaust-nozzle inlet
- c compressor
- i inlet to blade element
- j jet-nozzle throat
- o outlet of blade element
- t turbine

Relative Acceleration Rate

A brief, simple, quasi-static acceleration rate was calculated from the following assumptions:

- (1) Compressor efficiency η_c , pressure ratio P_3/P_1 , and corrected air flow $\frac{W\sqrt{\theta_1}}{\delta_1}$ obtained during steady-state operation of compressor are applicable during acceleration.
- (2) Turbine-nozzle area A_4 was constant and choked at all times $\left(\frac{W\sqrt{\theta_4}}{\delta_4A_4} = \text{constant}\right)$
 - (3) Turbine adiabatic efficiency $\eta_{t} = 0.85$.
 - (4) Turbine-inlet pressure $P_4 = 0.97P_3$.
- (5) Exhaust-nozzle area A_j was constant and static flight conditions prevailed $\left(\frac{W\sqrt{\theta_9}}{\delta_9 A_j}\right)$ a function only of $\frac{P_9}{P_1}$.

A turbine-inlet temperature ratio T_4/T_1 was calculated for several points along a constant corrected speed $N/\sqrt{\theta_1}$ line (65 percent rated speed) of a compressor map using continuity of flow between compressor inlet and turbine inlet:

$$\sqrt{\frac{T_4}{T_1}} = \left(\frac{0.97P_3}{P_1} \middle/ \frac{W\sqrt{\theta_1}}{\delta_1}\right) \frac{W\sqrt{\theta_4}}{\delta_4 A_4} A_4 \tag{1}$$

A pumping-characteristic curve $\left(\frac{P_9}{P_1}\right)$ plotted against $\left(\frac{T_9}{T_1}\right)$ was then obtained for each point using the defining equation for turbine efficiency

$$\frac{T_9}{T_1} = \frac{T_4}{T_1} \left\{ 1 - \eta_t \left[1 - \left(\frac{P_9}{P_1} \right) \frac{0.97 P_3}{P_1} \right)^{\frac{\gamma - 1}{\gamma}} \right] \right\}$$
 (2)

Another pumping-characteristic curve was also obtained from each point using continuity of flow between compressor inlet and exhaust nozzle:

$$\frac{P_9}{P_1} \frac{W\sqrt{\theta_9}}{\delta_9 A_j} = \frac{W\sqrt{\theta_1}}{\delta_1} \sqrt{\frac{T_9}{T_1}} \frac{1}{A_j}$$
 (3)

The intersection of the curves obtained from equations (2) and (3) gave the value of T_9/T_1 for each point during acceleration. The torque at a given point is equal to the moment of inertia multiplied by acceleration rate. It is also equal to the difference between turbine and compressor work divided by engine speed. The acceleration rate was calculated from torque for a constant moment of inertia I from the following equation:

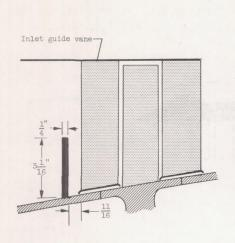
Acceleration rate =
$$\frac{\frac{W\sqrt{\theta_{1}}}{\delta_{1}}}{\frac{N}{\sqrt{\theta_{1}}}} \left\{ c_{p,t} \left(\frac{T_{4}}{T_{1}} - \frac{T_{9}}{T_{1}} \right) - \frac{c_{p,c}}{\eta_{c}} \left[\left(\frac{P_{3}}{P_{1}} \right)^{\frac{\gamma-1}{\gamma}} - 1 \right] \right\} (4)$$

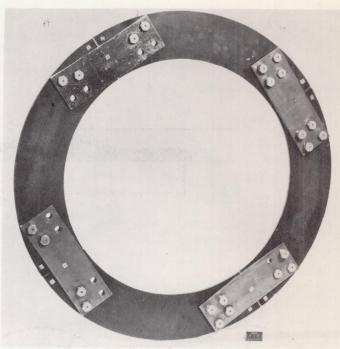
The relative acceleration rate was obtained by dividing the acceleration rate at each point by that obtained with no baffle at a turbine-inlet temperature ratio of 3.44.

The ratio of specific heats γ was assumed 1.40 for the compressor and 1.33 for turbine. Specific heat at constant pressure c_p was assumed 0.24 and 0.274 for compressor and turbine, respectively.

REFERENCES

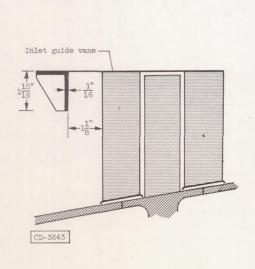
- 1. Huppert, Merle C., Calvert, Howard F., and Meyer, André J.: Experimental Investigation of Rotating Stall and Blade Vibration in the Axial-Flow Compressor of a Turbojet Engine. NACA RM E54A08, 1954.
- 2. Huppert, Merle C., Johnson, Donald F., and Costilow, Eleanor L.: Preliminary Investigation of Compressor Blade Vibration Excited by Rotating Stall. NACA RM E52J15, 1952.
- 3. Johnson, Donald F., and Costilow, Eleanor L.: Experimental Determination of Aerodynamic Forces Normal to the Chord Due to Rotating Stall Acting on Compressor Blading. NACA RM E54F14.
- 4. Huppert, Merle C., and Benser, William A.: Some Stall and Surge Phenomena in Axial Flow Compressors. Jour. Aero. Sci., vol. 20, no. 12, Dec. 1953, pp. 835-845.
- 5. Lucas, James G., Finger, Harold B., and Filippi, Richard E.: Effect of Inlet-Annulus Area Blockage on Over-All Performance and Stall Characteristics of an Experimental 15-Stage Axial-Flow Compressor. NACA RM E53L28, 1954.
- 6. Meyer, Andre J., Jr., and Calvert, Howard F.: Vibration Survey of Blades in 10-Stage Axial-Flow Compressor. II Dynamic Investigation. NACA RM E8J22a, 1949. (Supersedes NACA RM E7D09.)
- 7. Huppert, Merle C.: Preliminary Investigations of Flow Fluctuations
 During Surge and Blade Row Stall in Axial-Flow Compressors. NACA
 RM E52E28, 1952.

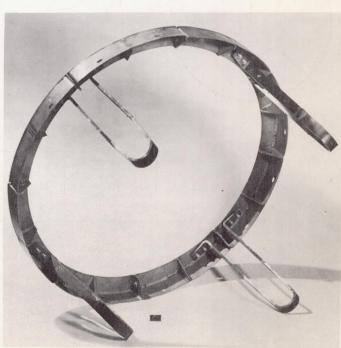




(a) Inside-diameter baffle. (33 percent area blockage).

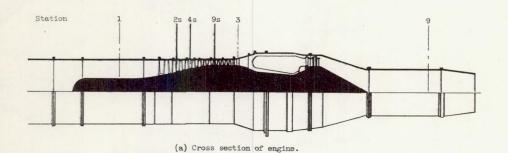
C-34193

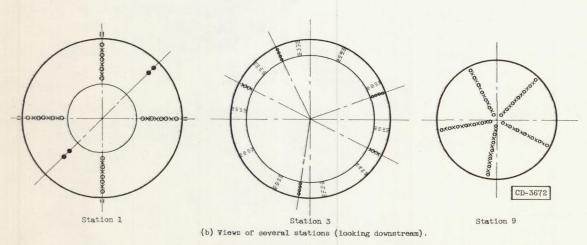




(b) Outside-diameter baffle. (33 percent area blockage). Figure 1. - Inlet-air baffles.

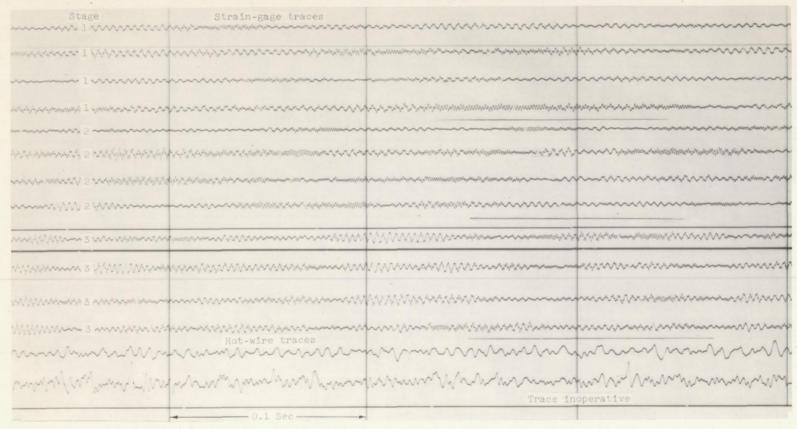
C-34191





| Symbol | Type of probe | | Station | | | | |
|--------|-------------------|----|---------|----|-----|-----|---|
| | | 1 | 2s | 4s | 9s | 3 | 9 |
| 0 | Total pressure | 20 | 5 | 5 | 3 | 12 | 3 |
| x | Total temperature | 12 | 5 | 5 | 3 | 6 | 3 |
| = | Wall static tap | 4 | - | - | - | - 1 | |
| | Stream static | 4 | - | - | - 1 | - 1 | |

Figure 2. - Cross section of engine showing stations at which instrumentation was installed.

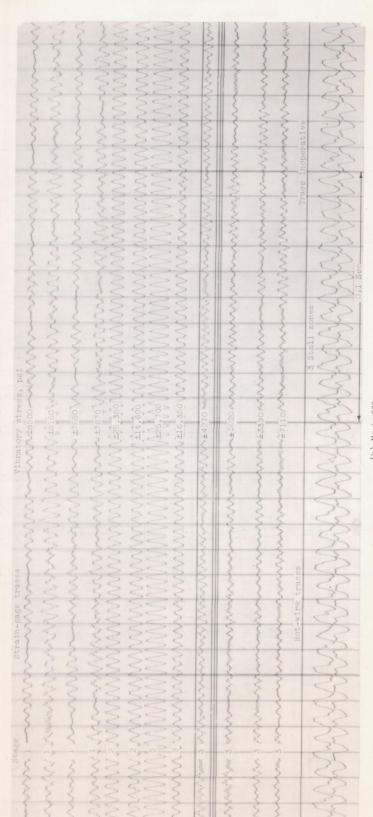


CONFIDENTIAL

(a) I.D. baffle. Stresses are between ± 1200 and ± 4719 pounds per square inch.

Figure 3. - Comparison of oscillograph records. Engine speed, 70 percent of rated speed.

3379



(b) No baffle. Forchuded. Comparison of oscillograph records. Engine speed, 70 percent of rated s

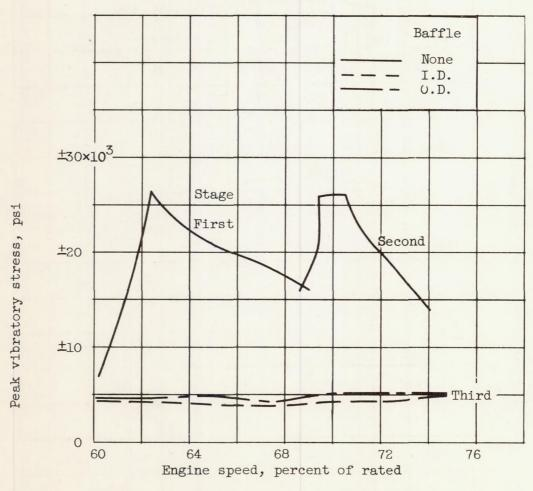


Figure 4. - Effect of inlet-air baffles on peak blade vibratory stress.

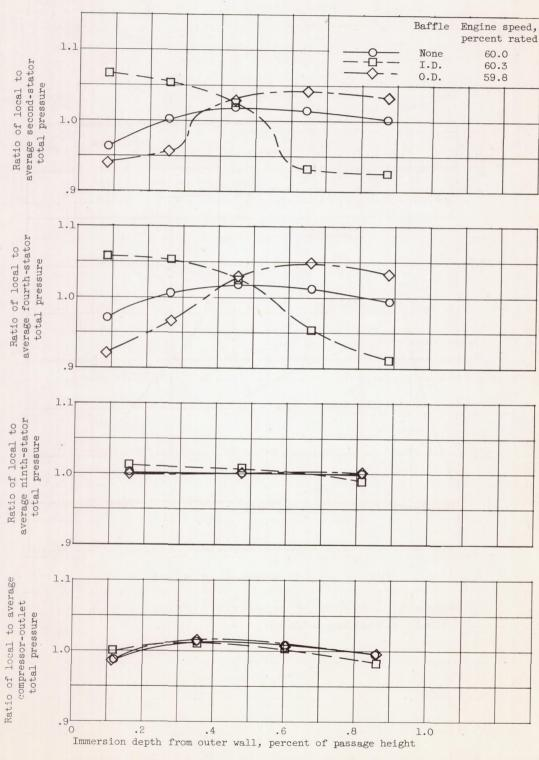


Figure 5. - Effect of inlet-air baffles on pressure profiles at several compressor stations.

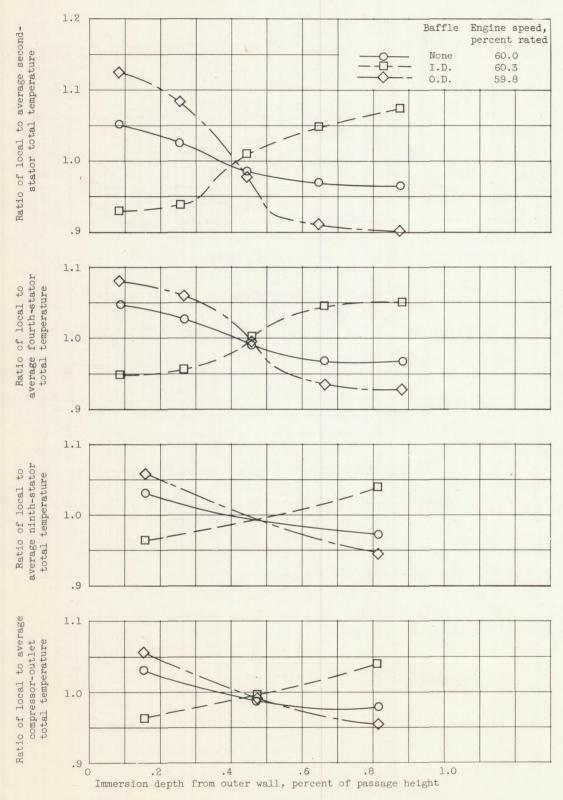


Figure 6. - Effect of inlet-air baffles on temperature profiles at several compressor stations.

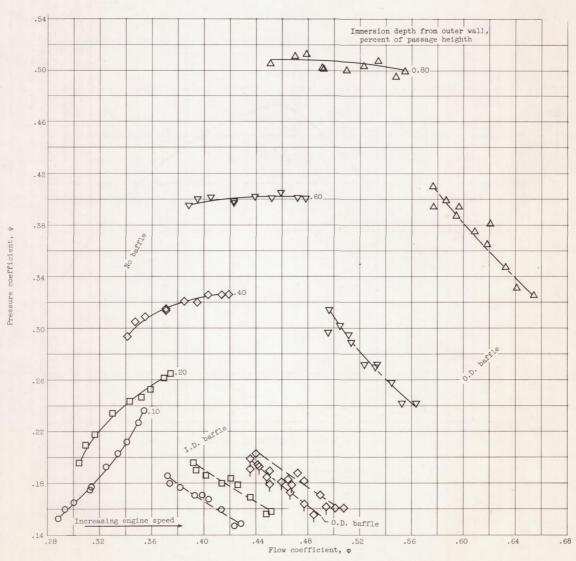


Figure 7. - Effect of inlet-air baffles on blade-element performance of first two compressor stages.

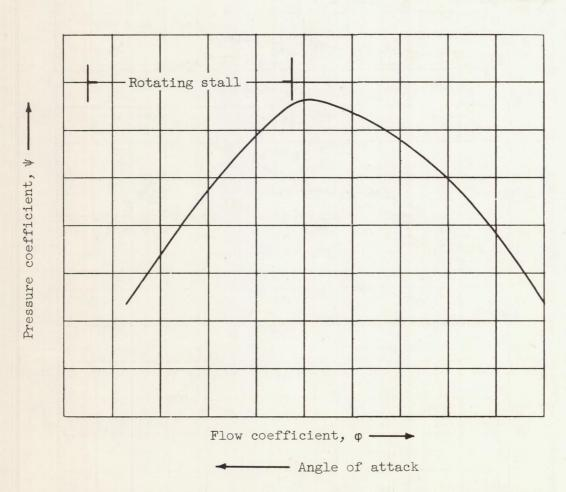


Figure 8. - Typical inlet-stage blade-element characteristic curve.

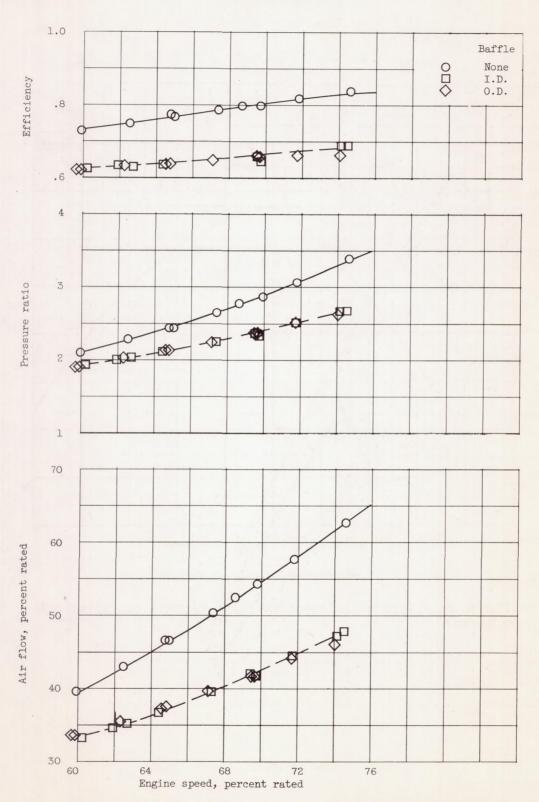


Figure 9. - Effect of inlet-air baffles on compressor performance as a function of engine speed; large exhaust-nozzle area.

CONFIDENTIAL

Pressure ratio

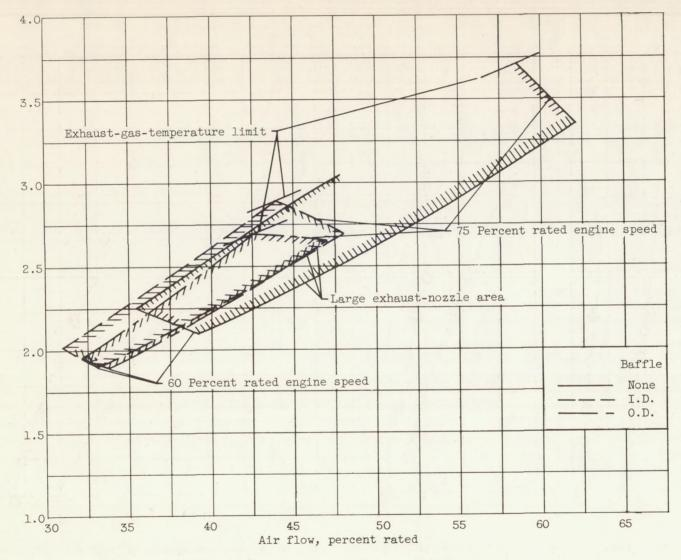


Figure 10. - Effect of inlet-air baffles on regions of compressor operation.

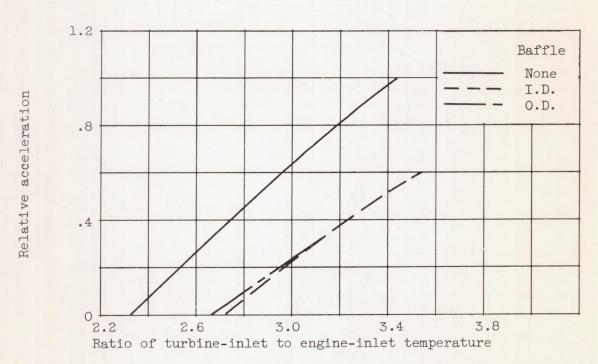
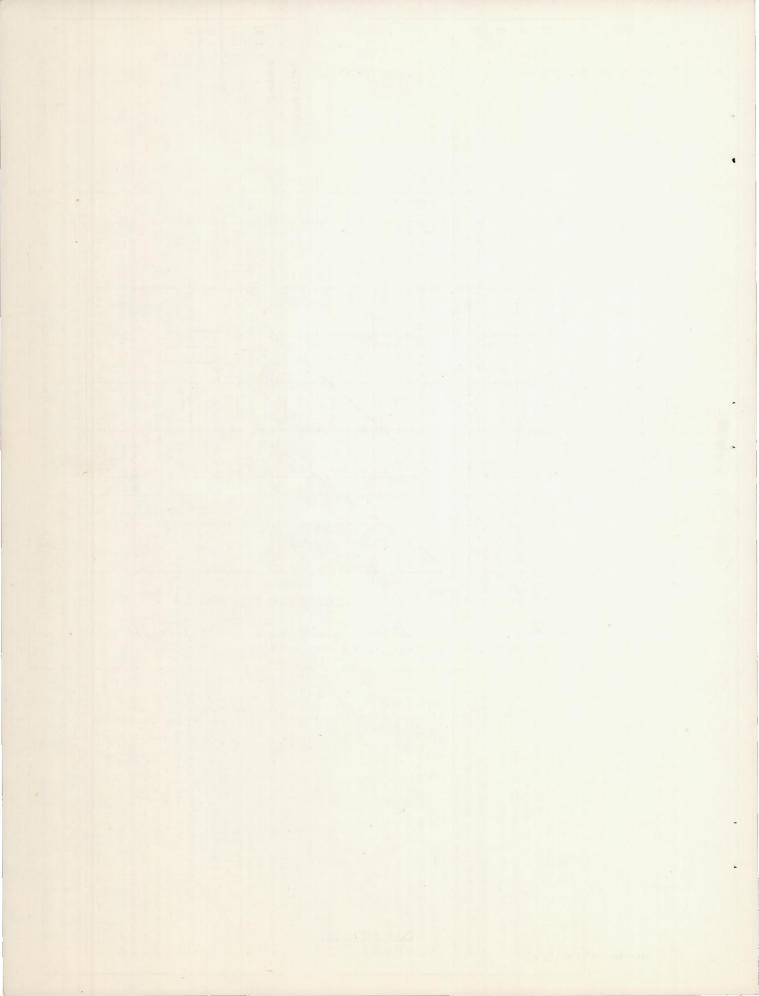
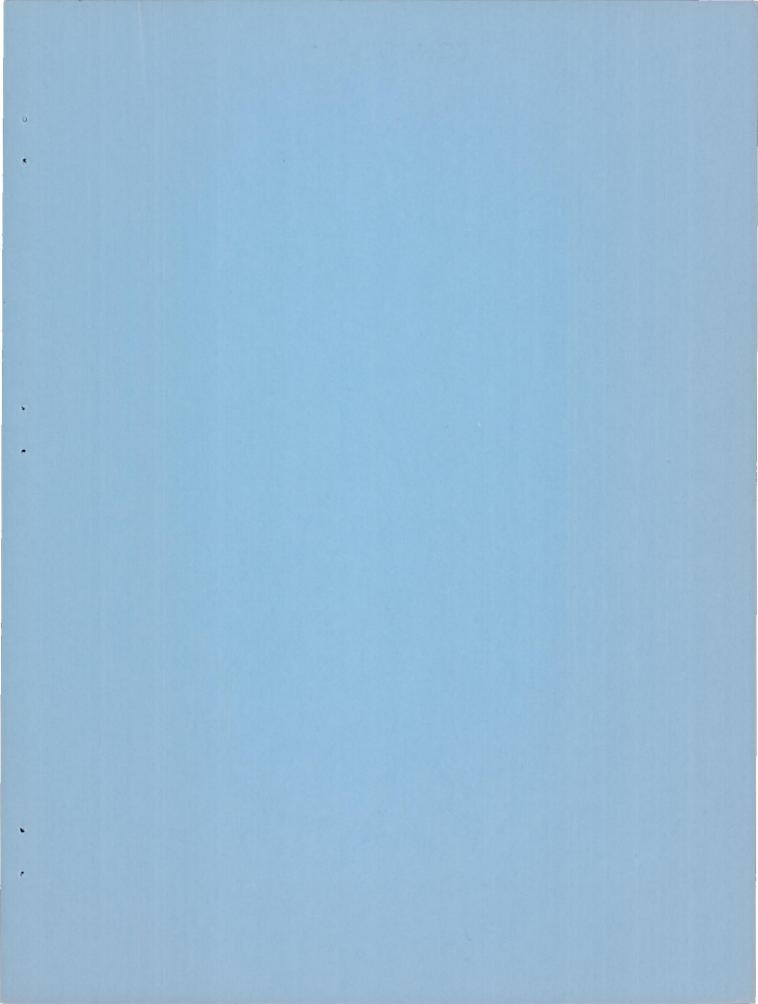


Figure 11. - Effect of inlet-air baffles on acceleration rate of engine; 65 percent rated engine speed.





CONFIDENTIAL

CONFIDENTIAL